

# Controller Design for a Limited Angle Torque Motor and dsPIC Implementation

Ilhami Çolak  
Faculty of Engineering and  
Architecture  
Istanbul Gelisim University  
Istanbul, Turkey  
icolak@gelisim.edu.tr

Murat Sahin  
Roketsan A. S.  
Mechatronic Design  
Department  
Ankara, Turkey  
msahin@roketan.com.tr

Semih Çakiroğlu  
Roketsan A. S.  
Mechatronic Design  
Department  
Ankara, Turkey  
scakiroglu@roketan.com.tr

Zafer Esen  
Roketsan A. S.  
Mechatronic Design  
Department  
Ankara, Turkey  
zesen@roketan.com.tr

**Abstract:** This study addresses the modeling of a LAT motor in Simulink environment and then designing and testing various controllers for this model. The LAT motor model is first expressed using equations which describe the DC motor dynamics. Then a simulation model is created using these equations. The non-linear part stemming from the limited torque angle of the motor is also added to the model. PID and cascaded PID controllers are designed for the model using classical design methods and parameters satisfying the design criteria are calculated. For testing the controllers on hardware using a real LAT motor, the controller codes are generated using Embedded Coder and embedded on a dsPIC microcontroller. The test data are then analyzed and the controller performances are evaluated.

**Keywords:** LAT motor, PID control, cascaded control, dsPIC controller implementation

## I. INTRODUCTION

DC motors are heavily used as actuators in systems with position controllers. They are used in systems ranging from robotics to industrial positioning. In mechatronic systems comprising position control, precision, repeatability and fast response times are a must [1]. To satisfy these requirements, limited angle torque (LAT) motors are also used. They are suitable for applications with mechanical angular limits. With their low volume, short response times and low inertia, they are preferred and used in aerospace and optics [2, 3]. As they have direct actuation capability, LAT motors don't need any transmission mechanism; so they allow more precise control and a volume advantage over traditional motors with transmission [3]. Some of the researches done about LAT motors are given below.

Y.Zhang and co. created a non-linear model of a LAT motor and they compared simulation and test results. They observed that the non-linear model approached the experimental results more closely [4]. Du Chunyang and co. used optimal control algorithms to drive a LAT motor in an optical scanning system. They used a DSP during their experiments [2]. F.S. Ahmed and co. used the LuGre friction model to obtain a non-linear model for the LAT motor. They drove the motor in open-loop and they compared the experimental results with the simulation results. They saw that the LuGre friction model

was suitable for modeling the mechanical dynamics of the motor [3].

In this study, position control of a LAT motor using various controller structures is done. A LAT motor is first chosen and modeled in MATLAB Simulink environment. Using the Control System Toolbox various controllers are designed. Control systems are evaluated using the motor model in MATLAB and controller parameters satisfying the requirements are obtained. Then an experiment system is prepared in the laboratory consisting of the modeled LAT motor and a dsPIC based controller and motor driver card. The controllers are tested using this setup and the data are saved. Lastly the results are compared and the control system which best satisfies the requirement is determined.

The usage of mechatronic systems are increasing by the development in DC motor technology. In recent years DC motors are preferred in some applications which need high power and high velocity rather than hydraulic and pneumatic systems because of their easy maintenance, easy usage and low cost properties.

In mechatronic systems LAT motors are in charge of translating electrical energy to the mechanical energy. Mechanical work comes true after triggering the motor by the control system and the new mission is defined by the feedback from the first work. Basic block diagram of a mechatronic system is given in Figure 1. In this diagram process can be either the missile system or a medical tool.

## II. LAT MOTOR MODEL

As the LAT motor is a DC motor, its electrical equation can be expressed as: [5]

$$E_a(t) = i(t)R + L \frac{di}{dt} + K_e \omega_m(t) \quad (1)$$

where  $E_a$  is the applied motor voltage,  $i$  is the phase current,  $R$  is the phase resistance,  $L$  is the motor inductance,  $K_e$  is the back-EMF constant and  $\omega$  is the rotor speed.

The mechanical equation of the motor can be expressed as:

$$\frac{d^2\theta_m(t)}{dt^2} = \frac{1}{J_m} T_m(t) - \frac{1}{J_m} T_l(t) - \frac{B_m}{J_m} \frac{d\theta_m(t)}{dt} \quad (2)$$

Where  $\theta_m$  is the rotor position,  $J_m$  is the rotor inertia,  $B_m$  is the viscous friction coefficient,  $T_m$  is the motor torque and  $T_l$  is the load torque.

Combining these equations the transfer function of rotor position with an input voltage is can be expressed as:

$$\frac{\theta_m(s)}{E_a(s)} = \frac{K_i}{LJ_ms^3 + (RJ_m + B_mL)s^2 + (K_eK_i + RB_m)s} \quad (3)$$

where  $K_i$  is the torque constant [6].

The limited angle of the motor was also considered in the model, and the model is built in Simulink environment as shown below in Fig. 1.

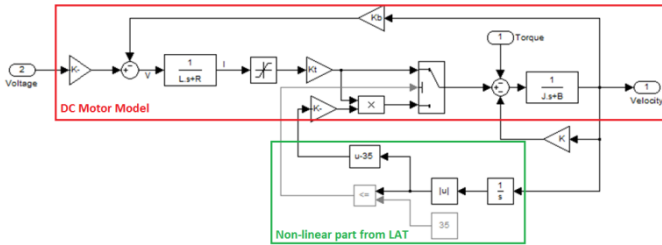


Fig. 1. LAT motor model in Simulink

The DC motor model is presented in the model as shown in the red rectangular part, and the non-linearity coming from the LAT motor is modeled as shown in the green part. As the motor torque starts to fall after the rotor moves away from the zero point by  $35^\circ$ , this non-linearity is modeled using a switch.

### III. POSITION CONTROL SYSTEMS

In feedback control systems design, the analysis of the open loop system is crucial for understanding how the closed loop system will behave. [7] In this regard, one of the most preferred methods is creating the root-locus curve and its analyzing it [8]. To obtain the root-locus curve, first the system transfer function must be obtained.

The root locus curve is calculated using (3) and the obtained graph is given below in Fig. 2.

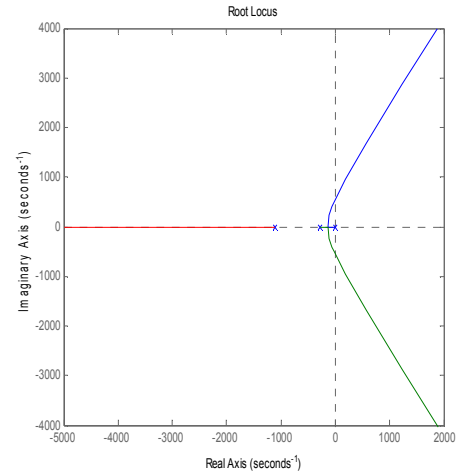


Fig. 2. Motor open-loop root-locus graph

As can be seen in the figure, the system has a total of three roots consisting of one root at origin, a second one near the origin (-285) and a third further one (-1115). The third root shows the electrical dynamics, the second root mechanical characteristics and the root at the origin shows the effect of the added integrator. The root coming from the electrical dynamics is much further than the one coming from the mechanical dynamics, thus mechanical dynamics will be much more dominant in the position response. A bandwidth of 10 Hz (63 rad/s) is determined as the requirement of the closed loop controller. The controller designs are done using this criterion.

Three controllers are designed to control the system:

- A PID position controller (Pos. controller),
- A cascaded PID position – velocity cascaded controller (Pos. Vel. controller),
- A position – velocity – current cascaded controller (Pos. Vel. Cur. controller).

#### A. Position Controller

The popular PID controller given in (4) is used as the main controller.

$$G_R(s) = \frac{U(s)}{E(s)} = K_p \left( 1 + \frac{1}{T_I(s)} + T_D(s) \right) \quad (4)$$

$E(s)$  is the error between the reference position command and the measured position. As can be seen, the controller adds two zeroes and a root to the system. Both of the zeroes can be positioned to the left or the root, or one of them can be placed on each side. As the zeroes shift to the left, the roots approach the imaginary plane and increase oscillation in the response. [9] The final system obtained by placing the roots and zeroes is given below in Fig. 3. The output of the Pos. controller is motor voltage.

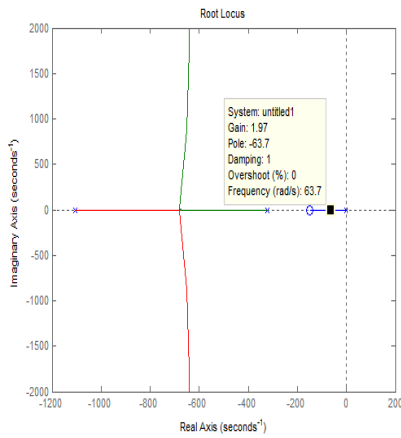


Fig. 3. Pos. controller closed-loop root-locus graph

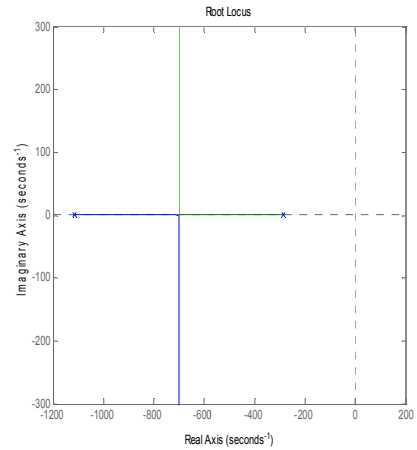


Fig. 5. Root-locus graph of the velocity controller

### B. Position-Velocity Cascaded Controller

A cascaded controller system consisting of an outer position control loop and an inner velocity control loop is used. The controller block diagram is given below in Fig. 4.

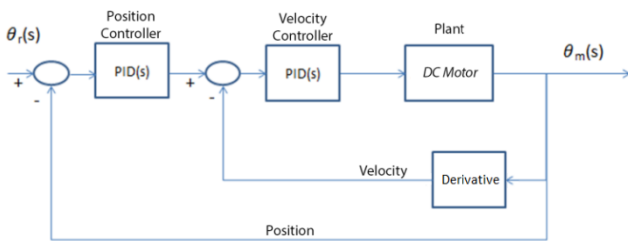


Fig. 4. Pos. Vel. controller block diagram

The position controller requirements are the system requirements. The velocity loop should be designed so that its bandwidth is theoretically at least two times the bandwidth of its outer loop. In practice however it's better to design it so that it has at least five times the bandwidth of its outer loop, so that the inner loop will not limit the dynamics of the outer loop. Increasing the bandwidth of the velocity loop too much will result in a very fast velocity response, but this will also increase the effect of disturbance caused by noise and quantization errors. [10] Considering these limitations, the bandwidth of the velocity loop controller is determined as 100 Hz.

The root-locus graphs for the velocity controller and the final position control system are given below in Fig. 5. and Fig. 6 respectively.

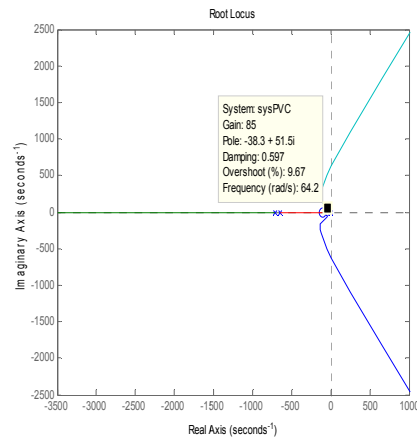


Fig. 6. Pos. Vel. controller closed-loop root locus graph

As can be seen in the figure, there aren't any routes at the origin, so a PI controller is required to prevent steady state error. The PI controller would add a root at the origin and a zero to the real axis. As part of the position control loop, as the velocity loop prevents the steady state error, only a P controller is satisfactory. A P controller gain is determined so that the outer loop bandwidth is 10 Hz.

### C. Position-Velocity-Current Cascaded Controller

In addition to the velocity controller loop mentioned in the previous section, a current controller loop is also added to the system which uses the phase current as its feedback. This makes it possible to control and limit the current dynamic of the system too. The block diagram of the Pos. Vel. Cur. controller system is given below in Fig. 7.

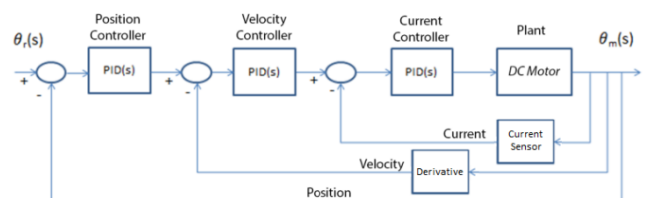


Fig. 7. Pos. Vel. Cur. controller block diagram

The bandwidth of the current controller loop is set to 500 Hz as to be 5 times the velocity controller loop. To design the controller, first the equation between the motor voltage and motor current is obtained as shown in (5).

$$\frac{i(s)}{E_a(s)} = \frac{J_m s + B_m}{JLs^2 + (B_m L + JR)s + (B_m R + K_e K_t)} \quad (5)$$

where  $i$  is the motor current,  $E_a$  is the motor voltage,  $J_m$  is the motor inertia,  $B_m$  is the viscous friction,  $L$  is the motor phase inductance,  $R$  is the motor phase resistance,  $K_e$  is the back-EMF constant and  $K_t$  is the torque constant.

The system consists of a zero which is very close to the origin and two roots. A PI controller must be used to prevent the steady state error. The PI controller will add to the system a root at the origin and a zero in the real axis. The root-locus graph of the current controller is given below in Fig. 8.

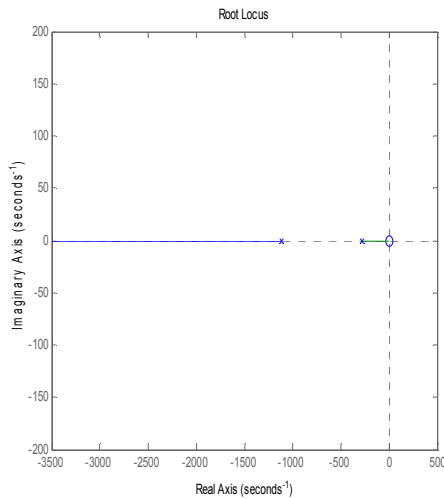


Fig. 8. Root-locus graph of the current controller

The velocity loop consists of three roots and a zero away from the origin. Again as the system doesn't have any free roots, a PI controller must be used to prevent steady state error. The PI controller will add a root at the origin and a real zero. At the required bandwidth, a simple P controller as the position controller is satisfactory. The root-locus graph for the final controller system is given below in Fig. 9.

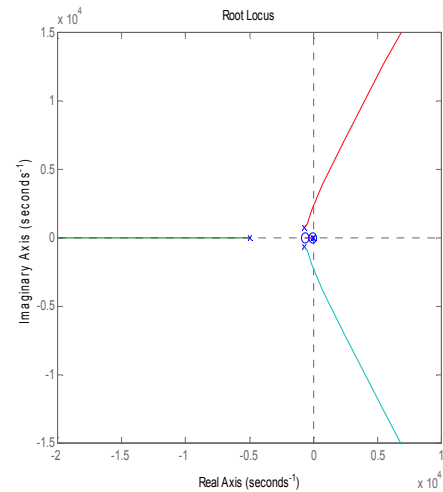


Fig. 9. Pos. Vel. Cur. controller closed-loop root locus graph

#### IV. HARDWARE IMPLEMENTATION AND DATA ACQUISITION

The test and data acquisition setup architecture is given below in Fig. 10.

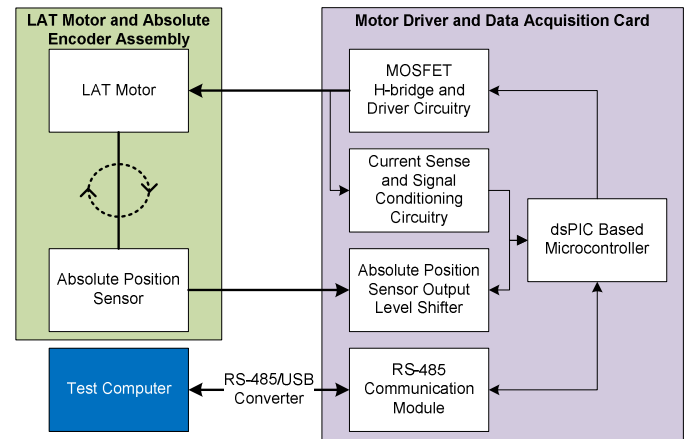


Fig. 10. Test and data acquisition setup architecture

The setup consists of three main parts. The first part is the LAT motor and an absolute position sensor assembly. The second part is an electronics card which drives the LAT motor, reads motor phase current and the absolute position sensor data, and outputs all of this data using RS-485 communication. The final part is the computer which is used for collecting and analyzing the data. The test setup is as shown below in Fig. 11.

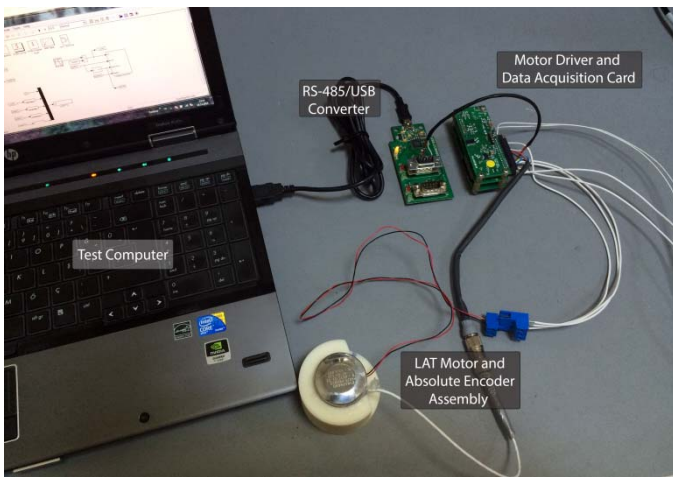


Fig. 11. Test and data acquisition setup

The controller algorithms are implemented on the motor driver card using the code generated from Simulink by Embedded Coder. The controller code is merged with the other firmware which handles the communication, motor drive and data acquisition. Then the resulting code is embedded into the dsPIC which is used as the microcontroller on the card.

## V. COMPARISON OF SIMULATION AND EXPERIMENTAL RESULTS

The three controllers are implemented on the test hardware and experimental results consisting of position, velocity and current measurements are collected in real time. Two reference signals are applied. The first one is a step command with an amplitude of 10 degrees. The second reference signal is a 10 Hz sine wave with an amplitude of 10 degrees.

The position responses of the three controllers for the step command are given below in Fig. 12.

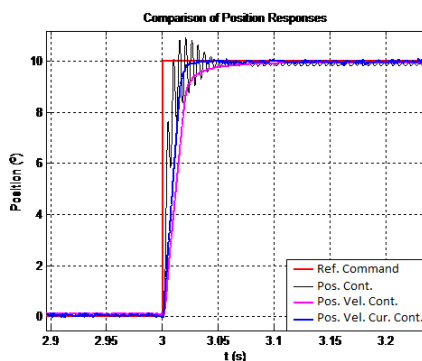


Fig. 12. Comparison of position responses, step command

In standard DC motors, although not always suitable in every application, a simple position controller would be enough. Due to the added inertia caused by the packaging, only feeding back and controlling the system using position data causes oscillations, as can be seen in the figure above. Adding

velocity and current dynamics to the system using cascade controllers is seen to be improving the controller rigidity according to the measurements. It can be seen in Fig. 12 that the controller with the current feedback has also the fastest response and best settling characteristics.

The velocity and current responses of the three controllers for the step command are given below in Fig. 13 and Fig. 14 respectively.

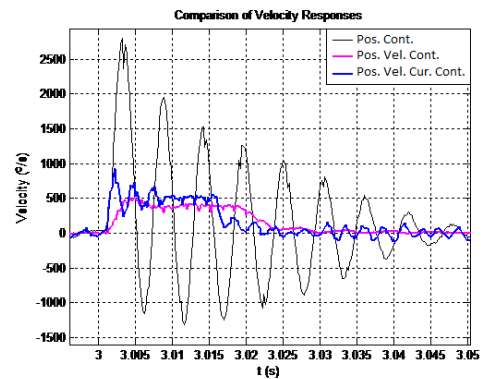


Fig. 13. Comparison of velocity responses, step command

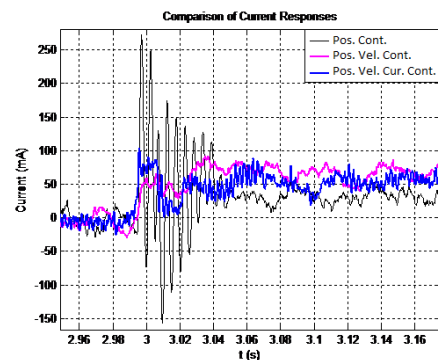


Fig. 14. Comparison of current responses, step command

It can be seen in Fig. 13 and Fig. 14 that the Pos. controller has the highest oscillations and as a result the highest power requirements. In the Pos. Vel. Cur. controller the velocity is observed to be faster and has some oscillations compared to the Pos. Vel. controller, but this also allows the faster response time in the position response.

The power requirements of the Pos. Vel. and Pos. Vel. Cur. controllers are roughly the same; however the Pos. Vel. Cur. controller requires slightly more current as it has a faster response.

The position responses of the three controllers for the sine wave signal reference are given below in Fig. 15.

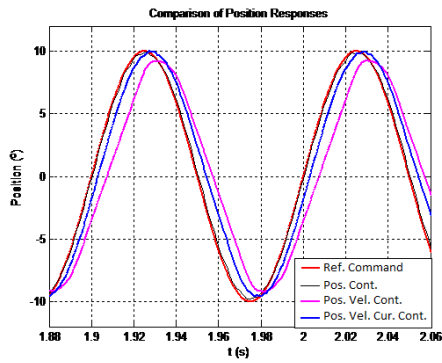


Fig. 15. Comparison of position responses, sine wave reference

It can be seen in the figure above that when a sine wave reference signal is applied as the command, Pos. controller also has an acceptable response. The Pos. Vel. controller is seen to have less bandwidth than the other two controllers.

The velocity and current responses of the three controllers for the sine wave reference are given below in Fig. 16 and Fig. 17 respectively.

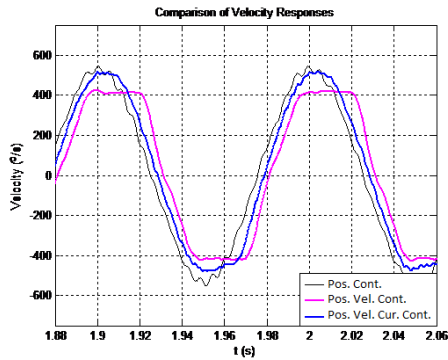


Fig. 16. Comparison of velocity responses, sine wave reference

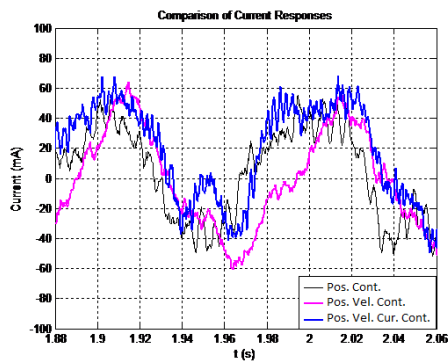


Fig. 17. Comparison of current responses, sine wave reference

The velocity and current responses are roughly the same in all three controllers, when a sine wave reference signal is applied as the input.

## VI. CONCLUSION AND FUTURE WORKS

In our study, the model of a LAT motor is implemented using its mathematical model in a simulation environment and three controllers are designed. First, the controller parameters are calculated in the simulation environment and then they are implemented and evaluated using test hardware.

As the experimental results show, the Pos. Vel. Cur. controller has the best overall performance considering the step and sine wave reference commands. The Pos. Vel. controller has the least oscillations, but falls short on bandwidth. The Pos. controller, although has good response characteristics when a sine wave reference is applied, has too much oscillations and a steep current demand when a step reference command is applied.

## APPENDIX

Motor parameters for the motor are given below:

$$J_m = 2.8 \text{ g.cm}^2, K_e = 0.021 \text{ V/rad/s}$$

$$K_t = 21.2 \text{ mN.m/A}, R = 7 \Omega, L = 5 \text{ mH}$$

## ACKNOWLEDGMENTS

Authors would like to thank Roketsan Co. for their financial support in this work.

## REFERENCES

- [1] N. Bacac, V. Slukic, M. Puškaric, B. Štih, E. Kamenar, S. Zelenika, "Comparison of different DC motor positioning control algorithms", MIPRO 2014, 26-30 May 2014.
- [2] Du Chunyang, Li Tiecai, Cao Zhengcai, "Accurate Tracking Control of a Limited Angle Torque Motor", Industry Applications Conference, 38th IAS Annual Meeting, 12-16 Oct. 2003
- [3] F. S. Ahmed, S. Laghrouche, M. El Bagdouri, "Nonlinear modeling of Pancake DC Limited Angle Torque Motor based on LuGre friction model", Vehicle Power and Propulsion Conference (VPPC), 1-3 Sept. 2010
- [4] Y. Zhang, I. R. Smith, and J. G. Kettleborough, "Performance Evaluation for a Limited-Angle Torque Motor", IEEE/ASME Transactions On Mechatronics, Vol. 4, No. 3, Sept. 1999
- [5] Nicolae Patrascoiu, "Modeling and Simulation of the DC Motor Using Matlab and LabVIEW\*", Int. J. Engng Ed. Vol. 21, No. 1, pp. 49-54, 2005.
- [6] Kiruthika, A., Rajan, A.A., Rajalakshmi, P., "Mathematical modelling and speed control of a sensed brushless DC motor using intelligent controller", Emerging Trends in Computing, Communication and Nanotechnology (ICE-CCN), 2013
- [7] Constantine H. Houppis, Stuart N. Sheldon, "Linear Control System Analysis and Design with MATLAB®, Sixth Edition (Automation and Control Engineering)", 2013.
- [8] Katsuhiko Ogata, "Modern Control Engineering (5th Edition)", Prentice Hall; 5 edition, September 4, 2009.
- [9] Benjamin C. Kuo, Farid Golnaraghi, "Automatic Control Systems", September 6, 2002.
- [10] Monteiro, J.R.B.A., Pereira, W.C.A., Santana, M.P., Almeida, T.E.P., Paula, G.T., Santini, I., "Anti-windup method for fuzzy PD+I, PI and PID controllers applied in brushless DC motor speed control", Power Electronics Conference (COBEP), 2013 Brazilian.